Acta Cryst. (1997). B53, 996–1005.

Packing Modes in Nitrobenzene Derivatives. II. The 'Pseudo-Herringbone' Mode

ISABELLE ANDRÉ, CONCEPCIÓN FOCES-FOCES,* FÉLIX H. CANO AND MARTIN MARTINEZ-RIPOLL

Departamento de Cristalografía, Instituto de Química-Física Rocasolano, CSIC, Serrano 119, E-28006 Madrid, Spain. E-mail: xconcha@roca.csic.es

(*Received 21 January 1997; accepted 4 August 1997*)

Abstract

Nitrobenzene derivatives pack in two main motifs: stacks [see André, Foces-Foces, Cano & Martinez-Ripoll (1997). *Acta Cryst.* B53, 984–995] and 'pseudo-herringbone' together account for some 61.5% of the structures classified as BCLASS = 15 by the Cambridge Structural Database. Several geometrical parameters allow the classification of the 'pseudo-herringbone' category into four main motifs. Weak interactions appear to play an important role in this packing mode.

1. Introduction

The simple shape of planar aromatic molecules allows, in principle, great freedom in their possible packing arrangements. However, among all the possible packing patterns, it is known that they pack in two main modes: in stacks or in a herringbone pattern (Gavezzotti & Desiraju, 1988; Desiraju, 1989; Desiraju & Gavezzotti, 1989*a*,*b*). It is widely recognized that structures which adopt the herringbone pattern are energetically and geometrically different from the stacked structures, whereas in the stacked structures the main stabilization is often through $\pi\cdots\pi$ interactions between neighbouring molecules (Gavezotti, 1990; Dahl, 1994). In the herringbone pattern the stabilization occurs mainly through $CH\cdots\pi$ interactions among a large number of non-parallel close neighbours (Sarma & Desiraju, 1985; Gavezzotti & Desiraju, 1988). The usual packing modes have been subdivided into four basic types as a function of the value of the shortest axis of the unit cell (SA) and of the value of the nearest neighbour interplanar angle (Gavezzotti & Desiraju, 1988; Desiraju, 1989; Desiraju & Gavezzotti, 1989*a*,*b*).

The present work is complementary to the preceding paper (André, Foces-Foces, Cano & Martinez-Ripoll, 1997) and deals with the packing of nitrobenzene derivatives in 'pseudo-herringbone' modes. The qualification 'pseudo' being necessary because the criteria given in the literature for herringbone types are not completely fulfilled. Indeed, the $\pi\cdots H$ interactions do not seem to be dominant in this mode, the molecules might not overlap in the 'backbone' direction and the range of SA values known for the herringbone patterns is not always respected; in some cases molecules are stacked, but the stacks themselves are organized in a herringbone fashion, with adjacent molecules making angles greater than 20°. We have used this interplanar angle value as a limit to distinguish the two patterns (simple stacks or 'pseudo-herringbones') because the short axis length (SA) criterion often used in the literature is not capable of discriminating between different modes of packing (Goddart, Haenel, Herndon, Krüger & Zander, 1995).

2. Methodology

2.1. *Database searches: geometrical characterization*

As in the preceding paper, crystallographic information on benzene nitro compounds was retrieved from the Cambridge Structural Database System (CSD Version 5.11, April 1996: Allen *et al.*, 1991) according to the conditions shown in Fig. 1 (André, Foces-Foces, Cano & Martinez-Ripoll, 1997).† Analysis of the geometrical parameters was carried out using the *VISTA* program (Cambridge Structural Database, 1995) and the *CERIUS*3.2 software (Molecular Simulations, 1993) running on a Silicon Graphics Indigo workstation.

The 'pseudo-herringbone' mode can be geometrically considered as stacks of aromatic rings in one or two directions (*x* or *y* in Fig. 1); these stacks group into slabs along a second (*z*) direction; grouping of these slabs generates the whole crystal. The motif within a slab is described through the distances *d*1, *d*2, *d*3 and *d*4 (Fig. 2) between ring centroids.

In order to investigate the arrangement of two consecutive motifs (*i.e.* the organization of the slabs), planes passing through the centroids of the molecules constituting the motif and related by translation operations [molecules labelled as (2) and (2′), and (1) and (1′) in Fig. 2] were defined as shown in Fig. 1. The interplanar distances (*d*, *I*1, *I*2, *I*3, *I*4 and *I*5) were evaluated using *CERIUS*3.2.

† A list of CSD refcodes, tables containing the geometrical parameters characterizing the arrangement of the slabs and those defining the slab, and the crystal packing diagrams of all the structures together with the histograms of the interactions have been deposited with the IUCr (Reference: BM0009). Copies may be obtained through The Managing Editor, International Union of Crystallography, 5 Abbey Square, Chester CH1 2HU, England.

2.2. *Intermolecular contacts: pattern description*

The existence of CH···π interactions has been investigated by defining intermolecular non-bonded contacts (Fig. 4) with the help of the *QUEST3D* (Cambridge Structural Database, 1994) program. All H atoms involved in non-bonded contact searches were placed in appropriate positions corresponding to their bond lengths as established from neutron studies (Allen *et al.*, 1987). Contact searches for non-bonded weak interactions involving O atoms of NO_2 groups as acceptors and C—H H atoms as donors were carried out and analysed in terms of the *d*O···H, *d*C···O and angular parameters, such as polar angles describing the elevation (θ) and rotation (φ) of the OH vector relative to the nitro plane containing the oxygen lone pairs.

3. Results and discussion

3.1. *Geometrical characterization*

A preliminary estimation of the similarities in their three-dimensional packing modes of the 169 entries allowed a first classification: 56 structures having at least two non-parallel aromatic rings (*i.e.* interplanar angles greater than 20°) were assigned to the 'pseudo-herringbone' mode.

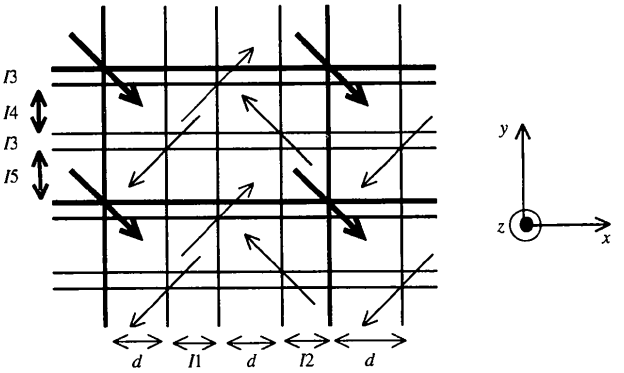

Fig. 1. Scheme showing the definition of the parameters used in the text: arrows represent oriented aromatic rings; lines represent the profile of planes through the centroids of related rings; the letters indicate the distances between these planes.

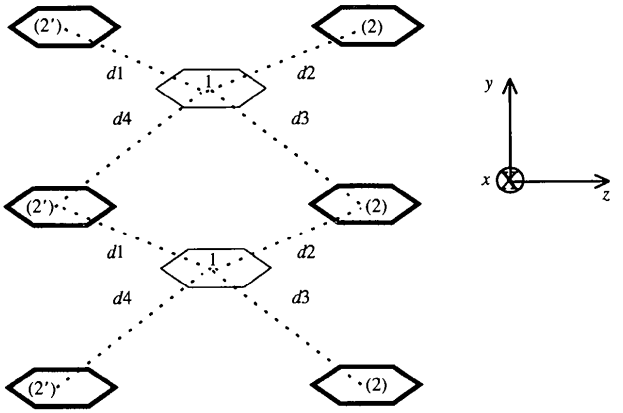

Fig. 2. Interaromatic ring centroid distances measured in the motif contained in a slab. Aromatic rings 2 and 2′ noted in bold are translation-related.

As with the stacked structures (André, Foces-Foces, Cano & Martinez-Ripoll, 1997), we have attempted to develop a geometrical method of classifying these 'pseudo-herringbone' structures: four main motifs have been established depending on the way in which the molecules (1 and 2) are located (Fig. 3): HB1 (subdivided into three subgroups: *a*, *b* and *c*, according to the orientation of the molecules in the motif), HB2, HB3 and HB4.

The HB1 type could be described as a regular and non-interrupted zigzag arrangement of aromatic rings visible on one of the structure projections. The pattern for HB2 may be derived from that of HB1 by translations of the aromatic rings along the *x* and *y* directions, as indicated in Fig. 3. The HB3 type is similar to HB2, the main difference being that in the former the basic motifs are alternately oriented in two opposite senses, whereas in the latter they are always oriented in the same sense (see Fig. 3). The HB4 motif is less defined than the previous types; it may be derived from the HB1(*c*) type by translation of the aromatic rings along the *y* direction; one example of each of the HB1, HB2, HB3 and HB4 structures (CSD refcodes: GASDOT, PNBZNT, LABVEP and FUDGOA) is given in Fig. 4.

Most of these 'pseudo-herringbone' structures allow the stacking of the aromatic rings. These stacks, schematized in Fig. 1, have been classified according to the description reported in the preceding paper (André, Foces-Foces, Cano & Martinez-Ripoll, 1997) and using the geometrical parameters with intercentroid distances in the range 0.0–6.0 Å (Table 1); slipped β-stacks (labelled B2 in the previous paper) are widely observed. In a second step of the packing description the relative position of a molecule [labelled as (1) in Fig. 2] with respect to its neighbouring molecules [labelled as (2)] constituting the 'pseudo-herringbone' motif and its three translation-related ones along two unit-cell axes [labelled as (2) and (2′)] has been analysed. Four general patterns have been observed, allowing a classification of the different packings types observed for the 'pseudo-herringbone' mode.

Type *A* is characterized by two equal adjacent distances ($d1 = d2$, $d3 = d4$) within the slab. Type *A*′ is a subcase of type *A*, where all the distances are equal ($d1 = d2 = d3 = d4$). Type *B* is characterized by equal opposite distances ($d1 = d3$, $d2 = d4$). Type *C* has two equal adjacent distances ($d1 = d4$, $d2 = d3$) in the direction of the motif axis. In all structures, a twofold screw axis is observed along the motif. Type *D* exhibits in two equal adjacent distances ($d1 = d4$) and two different ones ($d2/d3/d1$; Fig. 5). Type *D*′ corresponds to the same *D* type rotated by 90°. Type *E* is a subcase of type *A*, where the centroids *X*2′, *X*2 and *X*1′, *X*1 lie in the same plane (Fig. 6).

The structures are grouped independently of their space group (Tables 2–5), but according to the element of symmetry (glides, twofold screw axis and translation) relating the molecules constituting the motif.

In order to continue the crystal packing description, the arrangement of two consecutive slabs was studied; interplanar distances d, $I1$, $I2$, $I3$, $I4$ and $I5$, as described in the methodology paragraph (Fig. 1), were evaluated and are summarized in Tables 2–5. These parameters characterize the different 'pseudo-herringbone' types:

Type HB1 corresponds mainly to A or A' packing arrangements within the slab; it is characterized by short (1 Å) d and $I3$ values, and $I4 = I5$. The $I1$ and $I2$ values allow a distinction between HB1(a), HB1(b) and HB1(c);

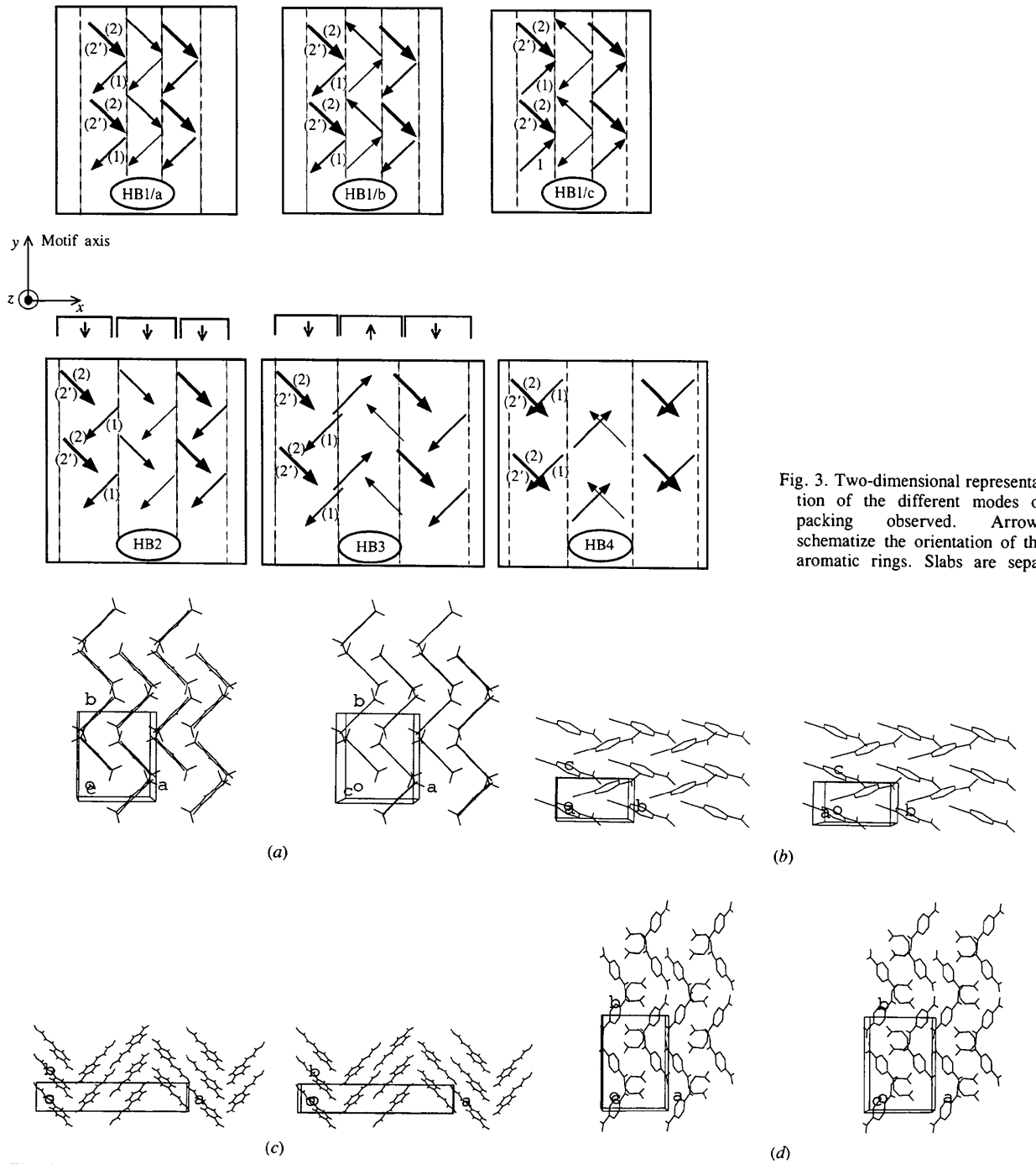

Fig. 3. Two-dimensional representation of the different modes of packing observed. Arrows schematize the orientation of the aromatic rings. Slabs are sepa-

Fig. 4. Stereo crystal packing views of (*a*) HB1 (1,3,5-trichloro-2,4-dinitrobenzene, CSD refcode: GASDOT), (*b*) HB2 (*p*-nitrobenzonitrile, PNBZNT), (*c*) HB3 (*p*-nitrocinnamic acid, LABVEP) and (*d*) HB4 structures [2-acetoxy-1-(4-nitrophenyl)ethanone, FUDGOA].

Table 1. *Geometric parameters observed for the stacks of the 'pseudo-herringbone' structures*

Refcode	*P*1*P*2 (°) *P*1*P*3 (°)	*X*1*X*2 (Å)	*X*1*X*3 (Å)	*X*1*P*2 (Å)	*X*3*P*1 (Å)	*X*2*X*3 (Å)	*X*3*P*2 (Å)	*X*213 (°)	*X*132 (°)	*DXY* (Å)	Overlap	Stacking group
HB1												
TNOXYL	0.0	5.74	5.74	3.93	3.93	11.48	7.86	180.0	0.0	0.00	W	*B2*
DCTNBZ	0.0	5.93	5.93	3.80	3.80	11.86	7.60	180.0	0.0	0.00	W	*B2*
BENCLN05	0.0	4.18	5.08	3.54	3.49	8.91	7.03	148.0	14.4	1.36	AR/AR	*N2c*/het
CMNBEN10	0.4	3.98	3.98	3.73	3.73	7.94	7.47	170.6	4.7	0.33	W	*N2b*/hom
NPCBNZ	0.0	5.02	5.02	3.76	3.76	10.05	7.51	180.0	0.0	0.00	W	*B2*
CNBZHM	0.0	4.24	3.70	3.70	3.57	7.55	7.26	143.9	19.3	1.24	AR/AR	*N2c*/het
KESNEB	0.0	5.73	5.73	3.58	3.58	11.46	7.15	180.0	0.0	0.00	W	*B2*
JULHED	0.0	3.95	5.46	3.60	3.70	9.18	7.31	154.5	10.7	1.23	AR/AR	*N2c*/het
MENBZS01	0.0	4.24	4.24	3.51	3.51	8.49	7.02	180.0	0.0	0.00	W	*B2*
GIMBOT	0.0	5.57	5.57	3.52	3.52	11.14	7.03	180.0	0.0	0.00	W	B2
GIMBOT	0.0	5.57	5.57	3.46	3.46	11.14	6.92	180.0	0.0	0.00	W	*B2*
HB2												
DNITBZ02	0.0	5.38	5.38	3.52	3.52	10.76	7.05	180.0	0.0	0.00	W	*B2*
DNITBZ02	0.0	5.67	5.67	2.81	2.81	11.34	5.62	180.0	0.0	0.00	W	*B2*
PNBZNT	0.0	3.85	3.85	3.45	3.45	7.69	6.89	180.0	0.0	0.00	W	*B2*
NIBZAL	0.0	3.96	3.96	3.62	3.62	7.92	7.24	180.0	0.0	0.00	W	*B2*
CLNIBZ01	0.0	5.29	5.29	3.36	3.36	10.58	6.73	180.0	0.0	0.00	W	*B2*
CLNIBZ01	0.0	5.93	5.93	2.66	2.66	11.86	5.32	180.0	0.0	0.00	W	*B2*
DNBENZ10	0.0	3.81	3.81	3.48	3.48	7.61	6.97	180.0	0.0	0.00	W	*B2*
HB3												
DEFDUN01	0.0	5.57	5.57	3.67	3.67	11.14	7.34	180.0	0.0	0.00	W	*B2*
NOPSFA	0.0	5.01	5.01	3.48	3.48	10.02	6.95	180.0	0.0	0.00	W	*B2*
NITBAL01	0.0	4.88	4.88	3.54	3.54	9.77	7.07	180.0	0.0	0.00	W	*B2*
LABVEP	0.0	5.03	5.03	3.48	3.48	10.06	6.96	180.0	0.0	0.00	W	*B2*
NPBUDO	0.0	3.86	3.86	3.48	3.48	7.73	6.96	180.0	0.0	0.00	W	*B2*
KOTHIK	0.0	5.76	5.76	2.89	2.89	11.51	5.79	180.0	0.0	0.00	W	*B2*
KOTHIK	0.0	5.26	5.26	3.68	3.68	10.51	7.35	180.0	0.0	0.00	W	*B2*
NIPHAZ	0.0	3.73	3.73	3.40	3.40	7.46	6.79	180.0	0.0	0.00	W	*B2*
HB4												
NITRB01	0.0	3.80	3.80	3.41	3.41	7.60	6.81	180.0	0.0	0.00	W	*B2*
DOXWIW	0.0	3.81	3.81	3.59	3.59	7.62	7.17	180.0	0.0	0.00	W	*B2*
NDMISF01	0.0	4.81	4.81	3.45	3.45	9.62	6.89	180.0	0.0	0.00	W	*B2*
CIGGEE	0.0	4.75	4.75	3.45	3.45	9.49	6.89	180.0	0.0	0.00	W	*B2*
MBZHIC	0.0	3.88	3.88	3.47	3.47	7.76	6.93	180.0	0.0	0.00	W	*B2*
VIFBER	0.0	3.83	3.92	3.47	3.39	7.05	6.86	130.4	24.5	1.63	AR/AR	*N2c*/het
KOTHEG	0.0	5.84	5.84	2.79	2.79	11.68	5.57	180.0	0.0	0.00	W	*B2*
KOTHEG	0.0	4.14	4.68	3.71	3.41	8.67	7.13	158.5	10.1	0.94	AR/AR	*N2c*/het
KODHUG	0.0	5.49	4.96	3.52	3.40	7.80	6.92	96.4	44.4	3.48	AR/S	*N2c*/het
BENCLN02	2.38	3.58	5.98	3.49	2.80	8.74	6.30	130.4	18.2	2.60	AR/S	*N2c*/het

PiPj (*i*,*j* = 1, 2, 3) represents the angle between planes *i* and *j*, which are equal in most cases, *XiXj* the distance between centroids *i* and *j*, and *XiPj* the average distance between the centroid *Xi* and its orthogonal projection on *Pj* and the centroid *Xj* on *Pi*. *Xijl* represents the angle between the vectors defined by the angle between the vectors defined by the centroids *XjXi* and *XjX*1. *Dxy* represents the offset of the aromatic rings along the stack. The abbreviations used to define the overlap are W: whole aromatic ring overlap; AR/AR: aromatic ring–aromatic ring overlap; AR/S: overlap involving aromatic rings and substituents.

Table 2. *Classification of the 'pseudo-herringbone' structures, HB1, according to the arrangement of the slabs*

Refcode	Space group	*I*1 (Å)	*I*2 (Å)	*I*4 (Å)	Pattern type	Type of packing
TNOXYL	*Pbcn*	5.69	5.69	2.87	*A'*	HB1(*a*) or HB1(*b*)
DCTNBZ	*Pbcn*	5.46	5.46	2.97	*A'*	HB1(*a*) or HB1(*b*)
NPCBNZ	$Pbn2_1$	4.90	4.90	2.51	*A'*	HB1(*a*) or HB1(*b*)
MENBZS01	$P2_1/n$	6.74	4.75	2.12	*A*	HB1(*c*)
BENCLN05	$P2_1/c$	4.60	4.31	3.25	*A*	HB1(*c*)
GASDOT	$P2_1/c$	4.76	4.79	4.18	*A*	HB1(*c*)
SAPYEN	$P2_1/c$	3.49	6.77	3.36	*A*	HB1(*c*)
CNBZHM	$P2_1/c$	3.60	3.95	3.12	*A*	HB1(*c*)
JAVGES	*Pbca*	3.35	6.74	3.84	*A*	HB1(*c*)
GIMBOT	$P2_1/c$	5.47	5.73	1.77	*A*	HB1(*c*)
KESNEB	*C*2/*c*	1.45	7.83	2.46	*A*	HB1(*c*)
JULHED	$P2_1/n$	4.59	4.59	2.46	*A*	HB1(*a*) or HB1/HB1(*a*)
SAWBIB	$P2_1/n$	4.20	4.20	2.65	*B*	HB1(*a*) or HB1(*b*)
CLNOBE02	$P2_1/a$	5.37	5.37	2.78	*C*	HB1(*a*) or HB1(*b*)
CMNBEN10	$Pna2_1$	3.33	3.33	4.16	*C*	HB1(*a*) or HB1(*b*)

whereas *I*1 and *I*2 values are equal for HB1(*a*) or HB1(*b*), these two values are different for HB1(*c*). Type HB2 corresponds mainly to the type *C* packing arrangement within the slab; it is characterized by *d* values greater than 1 Å; *I*3 values zero; *I*1 = *I*2 and *I*4 = *I*5. Type HB3 corresponds mainly to a type *C* packing arrangement within the slab; it is characterized by non-zero *d* and *I*3 values, *I*1 = *I*2 and *I*4 = *I*5. Type HB4 corresponds essentially to types *D* and *E* packing arrangements within the slab; it is characterized by zero values for *I*3, *I*1 = *I*2 and *I*4 ≠ *I*5. These characteristics are similar to those observed for the HB1(*c*) mode, after translation along the *y* direction and a rotation of 90° of the HB1(*c*) motif (see Fig. 3); it implies an interchange of the *I*1 and *I*2 parameters for the HB1 type with the *I*4 and *I*5 parameters defined for the HB4 type. One example of each type is represented in Fig. 4.

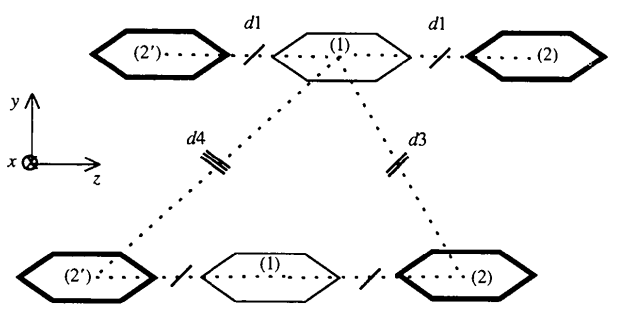

Fig. 5. Pattern type *D*.

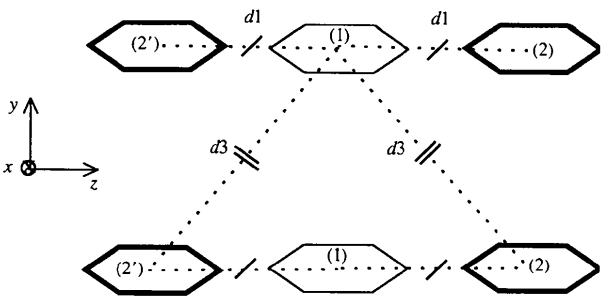

Fig. 6. Pattern type *E*.

Table 3. *Classification of the 'pseudo-herringbone' structures, HB2, according to the arrangement of the slabs*

Refcode	Space group	*d* (Å)	*I*1 (Å)	*I*4 (Å)	Pattern type
FOFCIM	$P2_1$	2.88	3.51	6.92	*C*
DNITBZ02	$P2_1/n$	5.47	5.47	2.70	*C*
PNBZNT	$P2_1$	1.61	2.24	3.53	*C*
NIBZAL	$P2_1$	3.09	4.48	1.98	*C*
DNBENZ10	$Pbn2_1$	3.48	3.54	1.90	*C*
CLNIBZ01	$Pna2_1$	5.18	5.39	2.64	*C*
GACFUL	*Pn*	2.79	5.62	4.87	*B*
HNIABZ20	$P2_1/c$	3.57	4.69	5.03	*D'*

3.2. *Description of the intermolecular contacts*

The herringbone pattern seems to be mainly governed by CH···π interactions (Sarma & Desiraju, 1985; Gavezzotti & Desiraju, 1988); for this mode, the average *X*1···H distance is in the range 3.1–3.2 Å (Albert de la Cruz, 1994); nevertheless, in the present study it appears that *X*1···H distances are centred around 3.9 Å and very few short distances around 3.1 Å are observed. Aromatic rings not involved in a common stack appear not to be overlapped in the projection along the motif axis (Figs. 2 and 3).

Other interactions may occur in this 'pseudo-herringbone' motif. As the common fragment of all the structures is a nitrobenzene, the possibilities of weak CH···O hydrogen interactions involving the NO_2 groups were analysed. CH···*X* hydrogen bonds have been the subject of extensive study (Sutor, 1963; Taylor & Kennard, 1982; Panunto, Urbanozyk-Lüpkowska, Johnson & Etter, 1987; Steiner & Saenger, 1992; Desiraju, 1995; Allen, Lommerse, Hoy, Howard & Desiraju, 1996) and the importance of weak CH···O interactions in the stabilization of some structures has been demonstrated (Sarma & Desiraju, 1986, 1987; Desiraju, 1991; Sharma & Desiraju, 1994). Among all

Table 4. *Classification of the 'pseudo-herringbone' structures, HB3, according to the arrangement of the slabs*

Refcode	Space group	*d* (Å)	*I*1 (Å)	*I*3 (Å)	*I*4 (Å)	Pattern type
DEFDUN01	$P2_12_12_1$	3.29	2.76	0.06	2.73	*C*
NOPSFA	$P2_12_12_1$	0.96	5.87	0.46	2.04	*C*
HADBOD	$P2_12_12_1$	3.18	1.55	1.10	2.75	*C*
NITBAL01	$P2_1/c$	5.47	6.92	0.22	2.22	*C*
LABVEP	$P2_1/a$	4.47	8.41	0.32	2.20	*C*
NPBUDO	$P2_12_12_1$	4.53	7.64	0.60	1.33	*C*
KOTHIK	$P2_12_12_1$	5.86	12.33	0.10	2.53	*C*
NIPHAZ	$P2_12_12_1$	5.26	3.77	0.79	1.08	*C*
KIFXIG	$P2_12_12_1$	2.29	2.44	1.04	2.06	*C*
LINNAX	$P2_12_12_1$	5.52	2.30	1.15	2.37	*C*
DTFNPS	$P4_12_12$	5.32	3.97	0.64	2.40	*C*
QQQHJA01	$P2_1/n$	4.45	3.85	0.27	3.44	*C*
GETFIU	$P2_12_12_1$	3.47	0.85	0.26	2.84	*C*
YOYVAJ	$P2_1/n$	0.47	10.43	1.87	2.38	*C*
DEJWIY	$P2_1/n$	3.25	4.46	1.34	2.56	*B*
DOHCUY	$P2_1/n$	3.86	3.45	2.47	3.03	*B*
HIBWUK	$P2_1/n$	2.40	3.01	0.12	4.61	*B*
JULGUS	$P2_1/n$	1.16	2.38	1.83	2.08	*B*
VEGBIS	$P2_1/a$	5.04	7.04	1.08	2.27	*D'*

Table 5. *Classification of the 'pseudo-herringbone' structures, HB4, according to the arrangement of the slabs*

Refcode	Space group	*d* (Å)	*I*1 (Å)	*I*4 (Å)	*I*5 (Å)	Pattern type
NITRBE01	$P2_1/c$	0.37	5.44	0.38	3.42	*D*
DOXWIW	$P2_1/c$	2.59	4.29	1.28	2.53	*D*
NDMISF01	$P2_1/c$	1.69	3.25	2.28	2.53	*D*
DEJWEU	$P2_1/a$	1.76	3.96	2.76	5.45	*D*
CIGGEE	$P2_1/c$	0.70	7.44	1.98	2.76	*D*
VIFBER	$P2_1/c$	5.00	0.37	3.80	3.25	*D*
KOTHEG	$P2_1/c$	0.27	4.06	0.20	5.64	*D*
KOWZAX	$P2_1/b$	0.00	3.59	2.94	5.23	*D*
SEYGUY	*Pbca*	0.95	3.80	1.40	2.69	*D*
FUDGOA	$P2_1/c$	5.92	0.35	5.55	3.46	*D*
KUMSOA	*Pbca*	1.86	3.54	2.53	2.66	*E*
MBZHIC	$Pca2_1$	4.76	5.77	0.62	3.25	*E*
KODHUG	*C*2/*c*	0.66	5.91	2.06	5.83	*E*
BENCLN02	*Pccn*	3.60	1.87	1.31	1.31	*E*

the 'pseudo-herringbone' structures, 228 contacts were obtained, with mean values for *d*O···H and *d*C···O of 2.7 (2) and 3.5 (2) Å, respectively, which are close to the sum of the corresponding van der Waals radii (Bondi, 1964). On the basis of distances alone, most of these contacts could not be described as significant interactions, but the distribution of the angles $|\varphi|$, $|\theta|$, N=O···H and O···H—C [mean values 137 (29), 29 (17), 126 (23) and 133 (20)°, respectively] show the existence of a preferred orientation for the contacts and suggests that the interaction, although weak, seems to play a significant role in packing (Sarma & Desiraju, 1986, 1987; Desiraju, 1991; Sharma & Desiraju, 1994). These interactions result in the formation of infinite chains of molecules. This fact has been shown to be important (Sharma & Desiraju, 1994) due to the cooperativity of intermolecular interactions for supramolecular assembly. There is a great variety of chain arrangements, but three major patterns have been observed that correspond to the *A*, *B* (Fig. 7) and *C* patterns previously described for the organization of the aromatic rings in the 'pseudo-herringbone' motif. Nevertheless, in two cases, NIPHAZ and LINNAX, the chain observed along the twofold screw axis is constituted by N···H or Cl···Cl interactions. Other hydrogen-bonding interaction arrangements, similar to those reported for *trans*-amides (Leiserowitz & Hagler, 1983; Etter, 1990; Bernstein, Etter & Leiserowitz, 1994), have been observed and correspond to the *A* and *B* patterns; these arrangements are mainly observed in the HB1 group.

In summary, the HB1 group follows a general pattern where molecules are associated by short C—H···O=N distances between the non-parallel aromatic rings to form chains which are themselves stacked. In a view of the HB2 and HB3 motifs the aromatic rings appear in most cases arranged head-to-head (*C* pattern) and each is translated with respect to its neighbour, since the *d* value is remarkably different from zero (*i.e.* the molecules are not organized in a single row such as for the *A* or *B* patterns of the HB1 group, where the *d* value is close to zero). The HB4 group appears more complex and shows no general tendency to form chains.

4. Bent structures mode

A total of 19 structures corresponding to compounds having at least two non-coplanar aromatic rings, bent due to the possibility of torsion around the inter-ring linkage, have a packing mode similar to the HB4 pattern described previously and, in a certain way, they could be considered as herringbone structures. Two different types are observed: Bent1 and Bent2 (Fig. 8). In the first type molecules are arranged in similar way to HB4, except that, in the present case, neighbour aromatic rings belong to the same molecule. The Bent2 type is

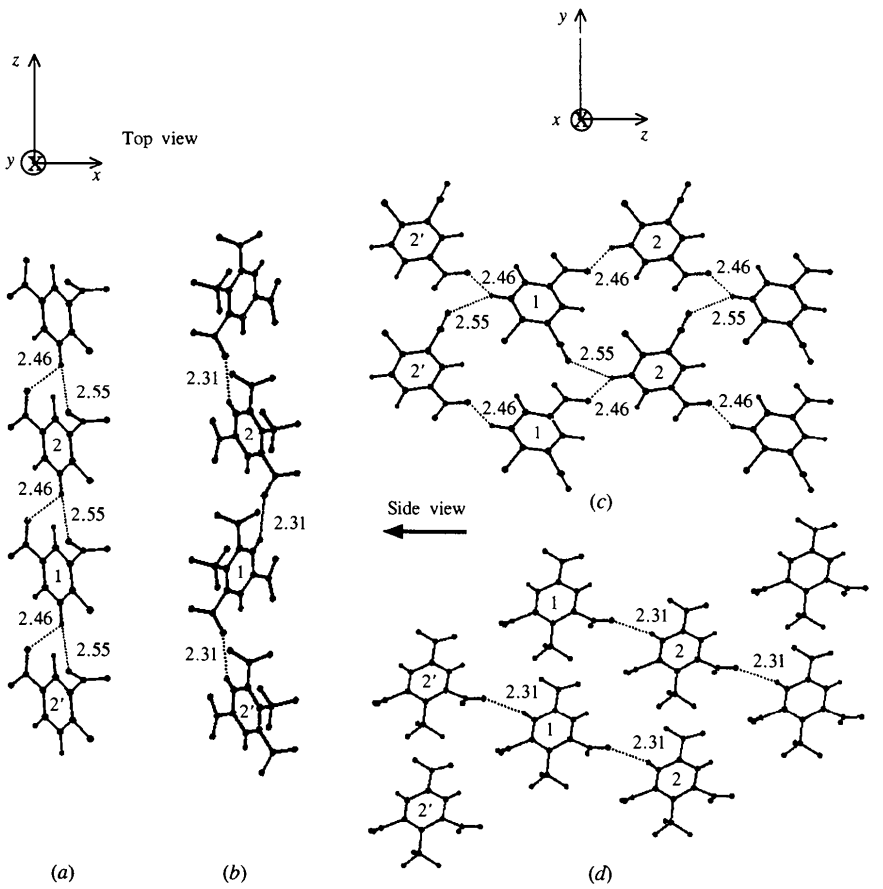

Fig. 7. C—H···O=N interaction chains observed for the *A* and *B* patterns. (*a*) and (*c*) down and side view of BENCLN05 (*β*-1-chloro-2,4-nitrobenzene) interaction chains (*A* pattern). (*b*) and (*d*) orthogonal views of SAWBIB (*α*,*α*,*α*-trifluoro-2,4,6-trinitrotoluene) interaction chains (*B* pattern). Axis orientation as in Fig. 3.

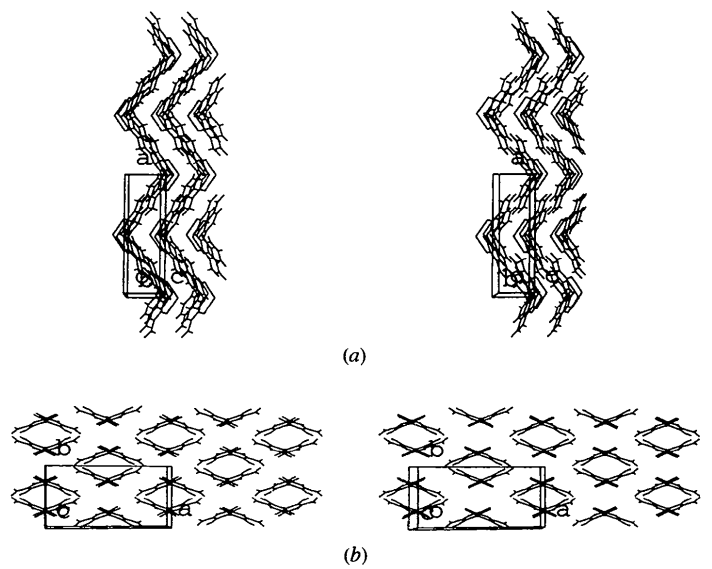

Fig. 8. Stereo crystal packing views of (*a*) Bent1 structures [CSD refcode: NBZSES: bis(*o*-nitrobenzeneselenyl)sulfide] and (*b*) Bent2 structures (CLNODL: 5,5′-dichloro-3,3′-dinitro-2,2′-biphenyldiol).

Table 6. *Geometrical parameters observed for the stacks of the bent structures*

Refcode	*P*1*P*2 (°) *P*1*P*3(°)	*X*1*X*2 (Å)	*X*1*X*3 (Å)	*X*1*P*2 (Å)	*X*3P^1 (Å)	*X*2*X*3 (Å)	*X*3*P*2 (Å)	*X*213 (°)	*X*132 (°)	*DXY* (Å)	Overlap	Stacking group
Bent1												
NBZSES	0.0	4.20	4.20	3.47	3.47	8.39	6.94	180.0	0.0	0.00	W	*B2*
CEGWUG	0.0	5.82	5.82	3.31	3.31	11.64	6.61	180.0	0.0	0.00	W	*B2*
EACBOZ	0.0	5.75	5.75	3.35	3.35	11.50	6.71	180.0	0.0	0.00	W	*B2*
BUDDAF	0.0	5.66	5.66	2.76	2.76	11.31	5.51	180.0	0.0	0.00	W	*B2*
SILTOW01	0.0	4.71	4.71	3.27	3.27	9.42	6.53	180.0	0.0	0.00	W	*B2*
Bent2												
ZZZJPA01	0.0	3.84	4.97	3.59	3.48	8.27	7.07	139.4	17.5	1.64	AR/AR	*N2c*/het
CLNODL	0.0	3.73	3.92	3.49	3.33	7.34	7.82	115.4	4.7	2.73	AR/S	*N2c*/het

Table 7. *Substitution pattern of simple nitrobenzene derivatives*

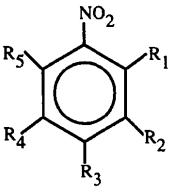

Refcode	R_1	R_2	R_3	R_4	R_5	Packing mode
Nitro-						
NITRBE01	H	H	H	H	H	HB4
CLNIBZ01	H	Cl	H	H	H	HB2
DOXWIW	Cl	Cl	H	H	H	HB4
NOMESL	CH_3	H	CH_3	H	CH_3	*N*2*a*/hom
HALJUZ	Pr^i	H	Pr^i	H	Pr^i	*N*2*c*/hom
PMNTBZ	CH_3	CH_3	CH_3	CH_3	CH_3	B2
Dinitro-						
ZZZFYW01	NO_2	H	H	H	H	*N*2*b*/hom
DEFDUNNO2	NO_2	H	Cl	H	H	Layer
DEFDUN01	NO_2	H	Cl	H	H	HB3
FULYEQ10	NO_2	CH_3	CH_3	CH_3	CH_3	*N*2*b*/het
DNBENZ10	H	NO_2	H	H	H	HB2
KIFXIG	H	NO_2	H	H	F	HB3
BENCLN02	H	NO_2	H	H	Cl	HB4
BENCLN05	H	NO_2	H	H	Cl	HB1
BAFLEZ	CH_3	NO_2	H	H	Cl	*N*2*c*/het
KUMSOA	H	NO_2	F	H	F	HB4
HIBWUK	H	NO_2	Bu^t	H	Bu^t	HB3
GASDOT	Cl	NO_2	Cl	H	Cl	HB1
DOHCUY	Bu^t	NO_2	CH_3	CH_3	CH_3	HB3
SAZHAC	CH_3	NO_2	CH_3	CH_3	CH_3	*N*2*a*/hom
DNITBZ02	H	H	NO_2	H	H	HB2
QQQECG01	Cl	Cl	NO_2	Cl	Cl	*B*2
Trinitro-						
SAWBIB	CF_3	NO_2	H	NO_2	H	HB1
CLNOBE02	Cl	NO_2	H	NO_2	H	HB1
DCTNBZ	Cl	NO_2	H	NO_2	Cl	HB1
TNOXYL	CH_3	NO_2	H	NO_2	CH_3	HB1
DOHCOS	CH_3	NO_2	Bu^t	NO_2	CH_3	*N*2*c*/hom
HECDOI	CH_3	NO_2	Br	NO_2	CH_3	*B*2

constituted by a motif similar to that of Bent1, the main difference being in the fact that in this case the basic motifs are alternate with an inverted equivalent. Stereoplots of two structures having these packing types are presented in Fig. 8 and the parameters defining these stacks are given in Table 6.

5. Molecular structure *versus* crystal structure

In order to study the influence of the nature and position of the substituents in the molecular structure on the packing mode, relatively simple nitrobenzene derivatives, bearing alkyl and halogen groups, were extracted from the set and the perturbation of the molecular structure on the crystal structure analysed. The substitution pattern of these 28 compounds is summarized in Table 7. In spite of the simplicity of the substituents, it appears that the comparison between them is somewhat difficult, but some relevant remarks may be made: in general, substitution by bulky groups (CH_3, Bu^t, Pr^i, NO_2) close to NO_2 influences the mode of packing, changing from a 'pseudo-herringbone' mode to a stack one. However, six exceptions to this tendency are observed (DEFDUN01 polymorph of DEFDUN, HIBWUK, QQQECG01, SAWBIB, TNOXYL and DOHCUY, representing 21% of the structures). An analysis of the coplanarity of the NO_2 group with the aromatic ring reveals a tendency for stacks for molecules to contain the non-coplanar NO_2 group with torsion angles around 90°, whereas with greater coplanarity we observe only the 'pseudo-herringbone' packing mode. These two points seem to indicate an influence of the NO_2 groups on the packing mode of these nitro compounds.

Comparison of a series of unsubstituted mono- and dinitrobenzenes (NITRBE01, ZZZFYW01, DNBENZ10 and DNITBZ02) reveals a tendency for these compounds to pack into a 'pseudo-herringbone' fashion: the exception is ZZZFYW01, probably for the reasons given previously regarding the influence of *ortho* substitution on the packing mode. The successive substitution of

these nitrobenzene derivatives seems to affect their mode of packing going from 'pseudo-herringbone' patterns to stacks, with totally substituted nitrobenzene derivatives (except DOHCUY) forming stacks. In a similar way, the influence of substitution on planar benzimidazolones has been observed (Schwiebert, Chin, MacDonald & Whitesides, 1996) and the mode of packing of these compounds has been shown to be drastically affected by the substitution due to a change in the shape of the benzimidazolone molecules. Furthermore, a homology in the mode of packing of the 1,3,5-trinitrobenzene derivatives (SAWBIB, CLNOBE02, DCTNBZ and TNOXYL) is observed. All these compounds pack in a HB1 'pseudo-herringbone' mode, similar to that observed for 1,3,5-trichloro-2,4-dinitrobenzene (GASDOT). When all substitution positions of these aromatic rings are occupied (DOHCOS and HECDOI), the tendency to form stacks, as described above, is observed.

6. Conclusions

Among the 169 structures analysed, it has been possible to classify 131 (77.5%) according to packing pattern similarities into four distinct general modes (stacks, layers, 'pseudo-herringbones' and bent structures). The remaining 38 structures do not apparently present common or well defined patterns. The most frequent groups in the 'pseudo-herringbone' mode can be grouped into different categories. The weak CH$\cdots\pi$ cloud of the phenyl rings and the C—H$\cdots$O=N interactions seem to govern this packing mode.

The comparative analysis presented here shows again that it is not an easy task to study crystal packing. The existence of polymorphism (DEFDUN and DEFDUN01; BENCLN02 and BENCLN05) shows that conditions of crystallization (thermodynamic kinetics, solvent *etc.*) are important; all these factors present obstacles to structural prediction.

Thanks are given to the Spanish DGICYT (PB93-0125) for financial support. One of us (IA) thanks the European Union for a grant (ERBCHRX-CT94-0469) under the Human Capital and Mobility program.

References

Albert de la Cruz, A. (1994). Doctoral thesis. Empaquetamiento molecular cristalino. University of Madrid, Spain.

Allen, F. H., Davies, J. E., Galloy, J. J., Johnson, O., Kennard, O., Macrae, C. F., Mitchell, E. M., Mitchell, G. F., Smith, J. M. & Watson, D. G. (1991). *J. Chem. Inf. Comput. Sci.* **31**, 187–204.

Allen, F. H., Kennard, F. H., Watson, D. G., Brammer, L., Orpen, A. G. & Taylor, R. (1987). *J. Chem. Soc. Perkin Trans. 2*, pp. S1–S19.

Allen, F. H., Lommerse, J. P. M., Hoy, V. J., Howard, J. A. K. & Desiraju, G. R. (1996). *Acta Cryst.* B**52**, 734–745.

André, I., Foces-Foces, C., Cano, F. H. & Martinez-Ripoll, M. (1997). B**53**, 984–995.

Bernstein, J., Etter, M. C. & Leiserowitz, L. (1994). *Structure Correlation*, edited by H.-B. Bürgi & J. D. Dunitz, Vol. 2, pp. 463–466. Weinheim, New York: VCH Publishers.

Bondi, A. (1964). *J. Phys. Chem.* **68**, 441–451.

Cambridge Structural Database (1994). *Getting Started with the CSD System. User's Manual.* Cambridge Crystallographic Data Centre, 12 Union Road, Cambridge, England.

Cambridge Structural Database (1995). *Vista*2.0 *User's Manual.* Cambridge Crystallographic Data Centre, 12 Union Road, Cambridge, England.

Dahl, T. (1994). *Acta Chem. Scand.* **48**, 95–106.

Desiraju, G. R. (1989). Editor. *Crystal Engineering. The Design of Organic Solids*, pp. 85–113. Amsterdam: Elsevier.

Desiraju, G. R. (1991). *Acc. Chem. Res.* **24**, 290–296.

Desiraju, G. R. (1995). *Angew. Chem. Int. Ed. Engl.* **34**, 2311–2327.

Desiraju, G. R. & Gavezzotti, A. (1989*a*). *Acta Cryst.* B**45**, 473–482.

Desiraju, G. R. & Gavezzotti, A. (1989*b*). *J. Chem. Soc. Chem. Commun.* pp. 621–623.

Etter, M. C. (1990). *Acc. Chem. Res.* **23**, 120–126.

Gavezzotti, A. (1990). *Acta Cryst.* B**46**, 275–283.

Gavezzotti, A. & Desiraju, G. R. (1988). *Acta Cryst.* B**44**, 427–434.

Goddart, R., Haenel, M. W., Herndon, W. C., Krüger, C. & Zander, M. (1995). *J. Am. Chem. Soc.* **117**, 30–41.

Leiserowitz, L. & Hagler, A. T. (1983). *Proc. R. Soc. London Ser. A*, **388**, 133–175.

Molecular Simulations (1993). *CERIUS*3.2. Molecular Simulations, Burlington, Massachusetts, USA.

Panunto, T. W., Urbanozyk-Lüpkowska, Z., Johnson, R. & Etter, M. C. (1987). *J. Am. Chem. Soc.* **109**, 7786–7797.

Sarma, J. A. R. P. & Desiraju, G. R. (1985). *Chem. Phys. Lett.* **117**, 160–164.

Sarma, J. A. R. P. & Desiraju, G. R. (1986). *Acc. Chem. Res.* **19**, 222–228.

Sarma, J. A. R. P. & Desiraju, G. R. (1987). *J. Chem. Soc. Perkin Trans. 2*, pp. 1195–1202.

Schwiebert, K. E., Chin, D. N., MacDonald, J. C. & Whitesides, G. M. (1996). *J. Am. Chem. Soc.* **118**, 4018–4029.

Sharma, C. V. K. & Desiraju, G. R. (1994). *J. Chem. Soc. Perkin Trans. 2*, pp. 2345–2352.

Steiner, T. & Saenger, W. (1992). *J. Am. Chem. Soc.* **114**, 10146–10154.

Sutor, D. J. (1963). *J. Chem. Soc.* pp. 1105–1110.

Taylor, R. & Kennard, O. (1982). *J. Am. Chem. Soc.* **104**, 5063–5070.